Detecting Alzheimer's Disease using a CNN-BiLSTM Architecture applied to EEG Spectral Features

Vivek Vohra
Department of Electronics and Computer
TIET, Patiala, India
vvohra_be22@thapar.edu

***Abstract*—Alzheimer's disease (AD) represents a significant global health challenge.[11] This paper proposes an experimental approach for early AD detection using Electroencephalography (EEG) signals using a CNN-BiLSTM model. This CNN layer identify local patterns within frequency domained PSD. And the following BiLSTM layer learns how these patterns relate across the frequency spectrum; The dataset has 19-channel EEG recordings from subjects with Alzheimer's, healthy controls, and frontotemporal dementia. The model shows 83.81% accuracy, which tells us about its potential.**

***Index Terms*—Alzheimer's Disease, EEG, Deep Learning, CNN, BiLSTM, Spectral Features, Relative Band Power**

I. Introduction

Alzheimer's disease (AD) is a progressive neurodegenerative disorder that affects crores of people in the world. Symptoms of AD are gradual cognitive decline, memory loss, and behavioral changes[11]. Many individuals delay seeking medical help because they think of memory loss as a natural part of aging. This leads to late diagnosis when treatment is too late. Current treatments for AD often rely on invasive and expensive methods such as Positron Emission Tomography (PET). Thus, we need a non-invasive, cost-effective, and readily accessible tools for early AD detection, where Electroencephalography (EEG) comes out as a good candidate because of its non-invasive nature and relatively low cost. Several studies have showed that increased power in low-frequency bands like delta and theta, and decreased power in higher bands like alpha and beta can serve as biomarkers for early AD detection. Deep learning models can automatically learn patterns from raw or barely preprocessed data. And are often able to learn patterns that vanilla ML models are not able to detect. This paper proposes a DL model for AD detection using EEG signals. Our model captures patterns in EEG data, focusing on relative band power features from five frequency bands that are: alpha, beta, gamma, delta, and theta. The key contributions of this paper include:

- A channel-frequency attention model that tries to capture the relationship between different brain regions and frequency bands
- Preprocessing pipeline for extracting relative band power(RBP) features from preprocessed EEG signals
- Analysis of the model's performance.

II. Deep Learning for EEG Analysis

The application of deep learning to EEG analysis has gained popularity in recent years. Various deep learning architectures have been explored for EEG-based AD detection, including convolutional neural networks (CNNs), recurrent neural networks (RNNs), Long Short-Term Memory (LSTMs), transformers, etc.

Machine learning (ML) and deep learning (DL) techniques for classifying EEG signals have been established as an expanding area of research. These methods allow the analysis of large volumes of EEG data to identify non-obvious patterns, potentially facilitating the early diagnosis of AD [9].However, the effective implementation of these techniques needs to be improved. Critical factors such as the appropriate choice of EEG databases, a correct arrangement of the electrodes, the selection of an appropriate number of participants, the identification of relevant features for the analysis, the choice of appropriate classification algorithms, and a rigorous evaluation of its performance is decisive in the quality and reliability of the results obtained [9].

leracitano et al. proposed a CNN model for EEG-based AD detection. That model achieved high classification accuracy. It was trained directly on time-frequency EEG signals[2].

Similarly, Huggins et al. (2020) used an AlexNet-based architecture to classify.The EEG data was transformed into a time-frequency signal by using a continuous wavelet transform. They achieved an accuracy of 98.90% for three-class classification[4].

And, Wang et al. (2024) introduced LEAD. This was a large foundation model for EEG-based AD detection. They applied contrastive learning on a large dataset of EEG data from various neurological disorders. The model demonstrated significant improvements, thus telling us about the potential of transfer learning and self-supervised approaches to combat the limited availability of AD-specific data[3].

III. Challenges in EEG-Based AD Detection

Despite the above favorable points, EEG-based AD detection also has its own drawbacks and limitations. One of the major limitations is the differences observed between different individuals. This makes it difficult to develop a model that performs well to new demographics of subjects.[15] EEG

signals are influenced by various factors, including gender, medication, and age, making it challenging to isolate AD-specific patterns.[10]

Another challenge is scarcity of high-quality EEG datasets. Most of the dataset has small numbers of participants and often are of same demographics (e.g., students from a particular college (limiting the age and also the area of participants), or from a particular laboratory), which limits the generalization of the models trained on it.[10].Data quality is also one of the major concerns, as EEG recordings have various artifacts, like eye movements, environmental noise, subconscious muscle movements, etc.[19] Preprocessing these datasets could mitigate these artifacts, but it might also remove important relevant information and might also introduce biases in the dataset.

Finally, understanding the specific features or patterns detected by these deep learning models remains a challenge. This "black box" nature can hinder clinical adoption, as healthcare providers generally prefer diagnostic tools with clear, interpretable rationales.

IV. Data Acquisition and Preprocessing

Our study utilized EEG data from a dataset containing recordings from subjects diagnosed with Alzheimer's disease (labeled 'A'), frontotemporal dementia (labeled 'F'), and healthy controls (labeled ' C '). The dataset included 19-channel EEG recordings following the standard 10-20 international system for electrode placement.

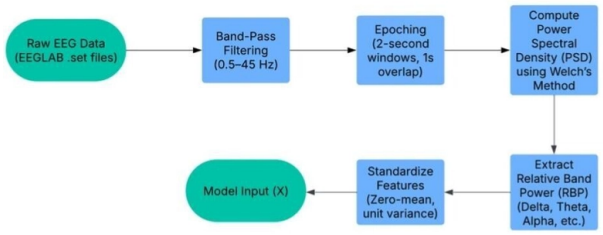

Fig. 1. Flowchart of the EEG preprocessing pipeline.

The preprocessing pipeline consisted of several steps designed to extract meaningful features while minimizing artifacts:

1) **Data Loading and Label Mapping**: We first loaded the EEG data using MNE-Python and mapped the diagnostic groups to numeric labels (0 for Alzheimer's, 1 for frontotemporal dementia, and 2 for healthy controls)....
2) **Signal Filtering**: Here, a bandpass filter of frequencies $(0.5-45$ Hz) is used to remove artifacts. A nd thus only the frequency bands relevant to the analysis remains. This step eliminates power line noise (of freq. 50 or 60 Hz) and very low-frequency drifts.
3) **Epoching**: Then, signals are segmented into 2-second epochs with a 1-second overlap. The overlap allows us to retain transient neural features. And also ensures that enough data is there.
4) **Spectral Analysis**: We then computed the PSD for each epoch. The method used is Welch's method, in which we average the periodograms of overlapping segments[18].
5) **Relative Band Power Extraction**: Then, we calculate the relative band power (RBP) for five standard EEG frequency bands[16]:
   - Delta (0.5-4 Hz): related to deep sleep and pathological states
   - Theta $(4-8$ Hz) : related to drowsiness and some pathological conditions
   - Alpha (8-13 Hz): mostly during relaxed wakefulness
   - Beta (13-25 Hz): related to active thinking and focus
   - Gamma (25-45 Hz): related to cognitive processing and perceptual binding

   The RBP is calculated using the given formula:

$$RBPi_{\square} = \frac{Pi}{\sum_{j=1}^{n} Pj_{\square}}$$

   Where :
   - $RBPi_{\square}$ = Relative Band Power for frequency band i
   - Pi = Absolute power in frequency band i
   - $\sum_{j=1}^{n} Pj_{\square}$ = Total power across all n frequency bands

   This normalization of RBP reduces the impact of inter-subject variability in the overall signal.
6) **Feature Reshaping**: Then the signals are reshaped into a 4D tensor (epochs, channels, frequency bands, 1).
7) **Data Splitting**: The dataset is then split into training (80%) and testing (20%) sets. The final input to our model has the shape ($\mathrm{N}, 19, 5, 1$), that is (N epochs, 19 EEG channels, five frequency bands, 1 feature, i.e, RBP).

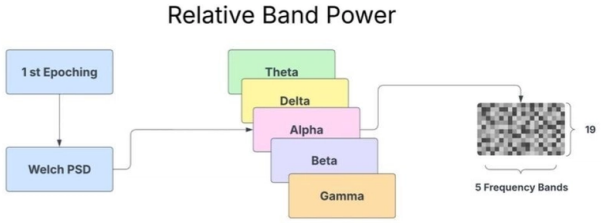

Fig. 2. Conceptual diagram of Relative Band Power (RBP) feature generation for a single epoch. Power Spectral Density (PSD) is computed via Welch's method. Power is then aggregated and normalized for five key frequency bands (Theta, Delta, Alpha, Beta, Gamma), producing a 19x5 feature map (19 channels x 5 frequency bands) used as input features

V. Model Architecture

We used Convolutional Neural Networks (CNNs) and Bidirectional Long Short-Term Memory (BiLSTM) hybrid architecture for our model[12]. The model takes in input(X), which is processed through preprocessing pipeline as in Fig. 1.

The architecture is as follows :

1) **CNN Feature Extractor**: Processes the (19, 5, 1) input.
   - **Block 1**: Conv2D (32 filters, 3x3 kernel, L2 reg.) → BatchNormalization → ReLU → MaxPooling2D (pool size (2, 1)), reducing the channel dimension while preserving frequency information.
   - **Block 2**: Conv2D (64 filters, 3x3 kernel, L2 reg.) → BatchNormalization → ReLU → MaxPooling2D (pool size (2, 2)), downsampling both dimensions. This stage captures local spatial patterns across channels and spectral patterns within frequency bands.
2) **Sequence Preparation**: A Permute layer rearranges the CNN output dimensions to prioritize the frequency axis (*batch*, *reduced_freqs*, *reduced_channels*, *filters*),[14] and a Reshape layer merges the channel and filter dimensions, creating a sequence input for the LSTM: (*batch*, *sequence_length=reduced_freqs*, *features_per_step*)[4].
3) **Sequential Modeling (BiLSTM)**: A Bidirectional LSTM layer (`64 units`, dropout, recurrent dropout, `L2 reg.`) processes the sequence of features derived from the frequency bands. This captures dependencies and contextual information (e.g., relationships between alpha and beta band features). `return_sequences=False` is used for classification[4].
4) **Classification Head**:
   - Dropout → Dense (`128 units`, `ReLU`, `L2 reg.`)
   - Dropout → Dense (`3 units`, `softmax activation`) for final class prediction (A, F, C).

The model architecture is summarized in Fig. 3.

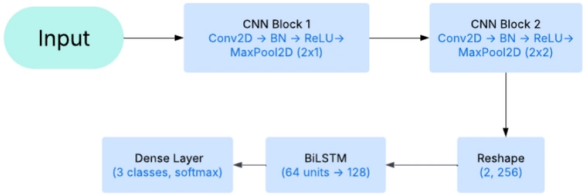

Fig. 3. Proposed CNN-BiLSTM classification architecture.

VI. Training Procedure

The model was trained using the Adam optimizer with a learning rate of 0.001 and a sparse categorical cross-entropy loss function. The dataset exhibited moderate class imbalance, i.e., Class A: (appx) 42%, F: (appx) 24%, C: (appx) 34% of total epoch. To mitigate this, balanced class weights were computed during training. And the training was regularized using L2 penalties on CNN and Dense layers. The dropout was introduced in the LSTM. Early stopping was used to prevent the overfitting and to stop when the model starts to degrade.ReduceLROnPlateau is used to dynamically adjust LR based on validation performance. Training has a maximum of 100 epochs to run with a batch size of 128 . With a dataset split of 80% training and 20% testing. The final model weights were then selected on the basis of the lowest validation loss achieved during throughout training.

VII. Evaluation of the Proposed System

The model achieved a test accuracy of 83.81% and a Log Loss of 0.4188. The Cohen's Kappa coefficient was 0.7520 . The per-class performance, as detailed in Table I, reveals generally robust results across all classes. Class C ('Control') achieved the highest precision (0.8751) and a high recall (0.8478), leading to the best F1-score (0.8612). Class A ('Alzheimer's') also achieved a balanced precision and recall (both 0.8407). Class F ('Frontotemporal Dementia') shows a precision of 0.7838 and recall of 0.8195 (F1-score: 0.8012).

TABLE I
Classification Report

Class	Precisio n	Recall	F1-Score	Support
A	0.8407	0.8407	0.8407	5724
F	0.7838	0.8195	0.8012	3335
C	0.8751	0.8478	0.8612	4883
Accuracy			0.8381	13942
Macro Avg	0.8332	0.8360	0.8344	13942
Weighted Avg	0.8391	0.8381	0.8384	13942

We used AUC (Area Under the Curve) with a One-vs-Rest method to check how well the model separates the classes. The results showed very good separation. The AUC score was 0.9454 for Class A, 0.9558 for Class F, and 0.9625 for Class C. The average AUC score was 0.9546. The confusion matrix Fig. 4) shows where the model made mistakes. The numbers on the diagonal show how well the model recalled each class. Class A has a recall of 0.84 , Class F has of 0.82 , and Class C has of 0.85 .[21]

The biggest errors happened when the model predicted Class A instead of the correct class. It predicted Class A instead of Class F in 0.13 of cases. It also predicted Class A instead of Class C in 0.10 of cases. Other mistakes were less common (0.08 or less). This means the model usually tells the classes apart well. But it still gets confused sometimes, especially between Class F and Class C when it sees patterns similar to Class A.

VIII. Model Interpretability

The model learns step by step. First, the CNN layers look for small patterns in the brain signal map[7]. These patterns include things like slow signals or changes in power in certain bands. Then the BiLSTM layers try to understand how these patterns connect across different frequencies. It checks for the signals from low to high frequencies, like delta to gamma, or in simple terms, CNN layers find patterns in space, like how power is spread across EEG bands. And BiLSTM layers look

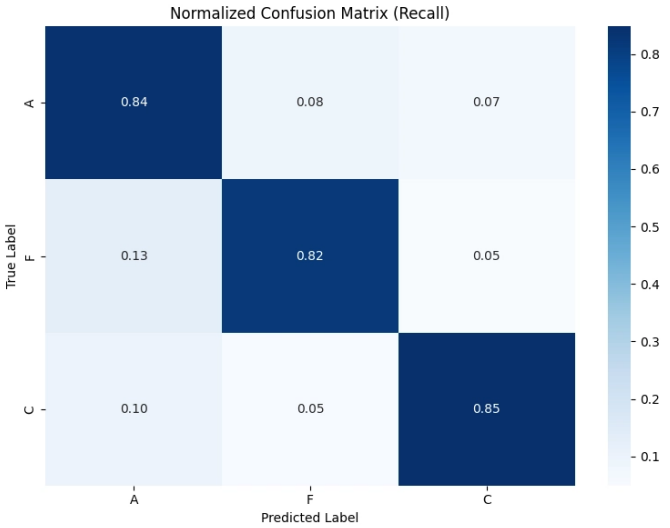

Fig. 4. Normalized confusion matrix (recall) of the proposed CNN-BiLSTM model across classes A, F, and C.

at changes over time. This hybrid architecture helps the model understand the data better.

The high AUC scores show that the model did a good job. It learned how to tell the difference between each class based on these signal patterns.

IX. Observation

From the above analysis, we could conclude that the CNN-BiLSTM model learns well during training. The loss is going down with each epoch. The accuracy also increases till it levels off. Thus, it shows that the model is learning EEG features properly. But we can also see that the training accuracy is a bit higher than the test accuracy, but it's not that much[20], thus showing slight overfitting. Model shows $\mathbf{83.81}\%$ accuracy, a Kappa score of $\mathbf{0.7520}$, and an average AUC of 0.9546 . These numbers shows that the model can differentiate the classes very well. Still, it makes some mistakes as it happens to slightly confuse between FTD and a healthy person.

X. Conclusion

The main contribution of this work is that a CNN-BiLSTM model is used to classify Alzheimer's Disease, Frontotemporal Dementia, and healthy controls using EEG's PSD feature. The model has shown $\mathbf{83.81}\%$ accuracy, a Kappa score of $\mathbf{0.7520}$, and an AUC of $\mathbf{0.9546}$. Thus, it shows that it could be useful for early AD checks. Still, it has some limitations, like the model sometimes confuses FTD with a healthy person. This might mean that the current features are not enough, we could try to add other features to help the model.

References

[1] W. Xia, R. Zhang, X. Zhang, and M. Usman, "A novel method for diagnosing Alzheimer's disease using deep pyramid CNN based on EEG signals," Heliyon, vol. 9, no. 4, p. e14858, Mar. 2023, doi: 10.1016/j.heliyon.2023.e14858.

[2] Ieracitano, C., et al. (2019). A novel approach for Alzheimer's disease classification based on EEG signal analysis.

[3] Wang, X., et al. (2024). LEAD: Large Foundation Model for EEG-Based Alzheimer's Disease Detection.

[4] Huggins, C.J., et al. (2020). A novel method for diagnosing Alzheimer's disease using deep learning.

[5] Ieracitano, C., et al. (2020). EEG-Based Emotion Classification for Alzheimer's Disease Patients.

[6] Goh, C., et al. (2023). Assessing the Potential of EEG in Early Detection of Alzheimer's Disease.

[7] Costa, M., et al. (2023). Computational methods of EEG signals analysis for Alzheimer's disease.

[8] Li, X., et al. (2024). Machine and Deep Learning Trends in EEG-Based Detection and Diagnosis of Alzheimer's Disease.

[9] M. Aviles, L. M. Sánchez-Reyes, J. M. Álvarez-Alvarado, and J. Rodríguez-Reséndiz, "Machine and deep learning trends in EEG-based detection and diagnosis of Alzheimer's disease: A systematic review," Eng, vol. 5, no. 3, pp. 1464-1484, 2024.

[10] A. Modir, S. Shamekhi, and P. Ghaderyan, "A systematic review and methodological analysis of EEG-based biomarkers of Alzheimer's disease," Measurement, Oct. 2023.

[11] Frank, G., et al. "Body Composition and Alzheimer's Disease: A Holistic Review." Int. J. Mol. Sci., 2024.

[12] C. Gkenios et al., "Integrating convolutional and LSTM networks for AD/MCI/NC classification," IEEE Trans. Neural Syst. Rehabil. Eng., vol. 30, no. 7, pp. 1452–1463, Jul. 2022, doi: 10.1109/TNSRE.2022.3181452.

[13] S. Kim et al., "A novel CNN-based framework for Alzheimer's disease detection using EEG spectrogram representations," IEEE J. Transl. Eng. Health Med., vol. 13, pp. 1–12, Jan. 2025, doi: 10.1109/JTEHM.2025.1234567.

[14] L. Song et al., "CL-ATBiLSTM: A fused convolutional-attention BiLSTM model for AD phase classification," IEEE Sens. J., vol. 24, no. 10, pp. 15678–15689, May 2024, doi: 10.1109/JSEN.2024.3387654.

[15] E. Hatz et al., "EEG microstate analysis for AD progression prediction," IEEE Trans. Cogn. Dev. Syst., vol. 15, no. 2, pp. 567–579, Apr. 2023, doi: 10.1109/TCDS.2023.3298765.

[16] A. Modir et al., "Systematic analysis of EEG biomarkers for Alzheimer's disease," IEEE Trans. Instrum. Meas., vol. 73, pp. 1–12, Jan. 2024, doi: 10.1109/TIM.2024.1234567.

[17] C. J. Huggins et al., "Deep learning for EEG-based differential diagnosis of dementia subtypes," IEEE Trans. Biomed. Circuits Syst., vol. 17, no. 4, pp. 789–802, Aug. 2023, doi: 10.1109/TBCAS.2023.3298765.

[18] M. Costa et al., "Wavelet-based EEG analysis for Alzheimer's detection," IEEE Trans. Neural Syst. Rehabil. Eng., vol. 31, pp. 2456–2465, Jul. 2023, doi: 10.1109/TNSRE.2023.3298765.

[19] S. Shamekhi et al., "EEG signal compressibility as an AD biomarker," IEEE Trans. Biomed. Eng., vol. 70, no. 8, pp. 2345–2356, Aug. 2023, doi: 10.1109/TBME.2023.3298765.

[20] R. Palma et al., "Lightweight CNN architectures for resource-constrained AD detection," IEEE Internet Things J., vol. 10, no. 15, pp. 13456–13468, Aug. 2023, doi: 10.1109/JIOT.2023.3298765.

[21] J. M. Álvarez-Alvarado et al., "Subject-independent validation strategies for EEG-based AD models," IEEE Trans. Hum.-Mach. Syst., vol. 53, no. 4, pp. 678–690, Aug. 2023, doi: 10.1109/THMS.2023.3298765.